Hindawi
Journal of Chemistry
Volume 2022, Article ID 2376597, 11 pages
https://doi.org/10.1155/2022/2376597

Research Article

Experimental Design and Optimization of Decolourization of Reactive Black-5 Dye Using Cloud Point Extraction

Sathish Kumar Ramachandran[1], **Leta Deressa Tolesa**[2], **Mohammedsani Abdulkadir Aba Gissa**[3], **and Duraimurugan Alias Saravanan Dhanabalan**[3]

[1]*Department of Biomaterials, Saveetha Dental College and Hospitals, Saveetha Institute of Medical and Technical Sciences, Saveetha University, Chennai 600077, India*
[2]*Department of Chemistry, College of Natural & Computational Sciences, Mettu University, Oromia, Ethiopia*
[3]*Department of Chemical Engineering, Mettu University, Metu Zuria, Ethiopia*

Correspondence should be addressed to Duraimurugan Alias Saravanan Dhanabalan; duraisaran31@gmail.com

Received 7 December 2021; Revised 20 April 2022; Accepted 23 August 2022; Published 26 September 2022

Academic Editor: Gomaa A. M. Ali

A two-phase separation method called cloud point extraction (CPE) does not use hazardous or flammable organic solvents. The efficient removal of the dye Reactive Black-5 (RB-5) from an aqueous solution using Triton X-114, a nonionic surfactant, is described in this study. Three-level factorial design and response-surface methods were used to quantify the impact of process variables on the CPE process, such as operating temperature and surfactant concentration. Investigations were conducted into how these process variables affected the ratio between the phase volumes, the concentration of dye in the surfactant-rich phase, and the residual amounts of dye in the diluted phase. As a result, ANOVA was used to create and validate mathematical models. The findings demonstrated that the correlation coefficients (R^2) exceeded 0.98. The acquired findings showed that the suggested extraction process is efficient, and the proposed CPE approach removes 98% of the RB-5 dye under optimal conditions.

1. Introduction

The delicate environment is threatened by significant amounts of colored organic effluents from diverse textile companies. The remaining dyes make up 1–15% of the colored wastewater that is dumped into water bodies [1]. Nearly 10,000 dyes and coloring chemicals are used exclusively by the textile industry [1, 2]. These substances and pigments are still present in the ecosystem and have a negative impact on nature and all living beings in different ways [3, 4]. They reduce the diversity of aquatic creatures and plants by preventing sunlight from accessing the water bodies [5, 6]. Due to their brightness and durability, reactive dyes outperform other dyes in the dyeing of cellulose fibers [7]. Reactive Black-5 (RB-5) is a dye that belongs to the diazo category. It is broadly applied in the paper, leather, and textile industries. 15% of the dyes used in the textile industry are lost in the dyeing process's effluent [8]. The most significant pollutants in textile wastewater are dyes, as well. As a result, RB-5 was chosen as the model dye for textile effluent in this study.

Utilizing a variety of techniques, including nanofiltration [9], adsorption on solid agricultural waste [10], micellar-enhanced ultrafiltration [11], adsorption with bentonite clay [12], ozonation [13], oxidation [14], activated carbon adsorption [15], and surfactant impregnated with aluminum-rich montmorillonite clay [16], among others, the decolorization of textile effluents is accomplished. Every one of the aforementioned techniques has benefits and drawbacks. Both ultrafiltration and nanofiltration have excelled in their respective fields. However, due to membrane fouling, which drastically decreases permeate flux and membrane life, their use is restricted [8, 10]. Due to the fact that dyes are not easily biodegradable, typical wastewater treatment procedures are unable to effectively remove them [17].

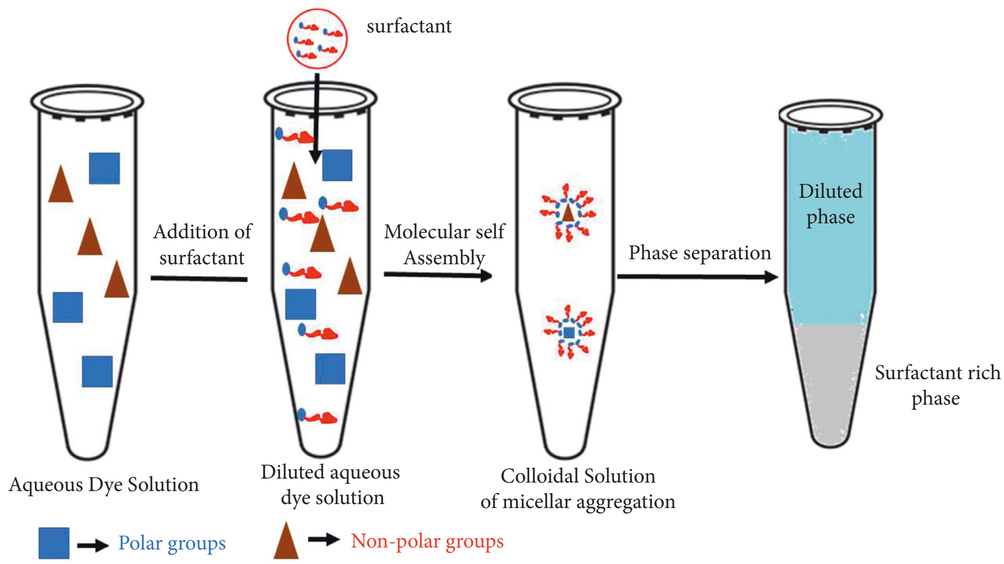

Figure 1: Structure of Reactive Black-5 dye.

Because it does not require organic solvents for liquid-liquid extraction, a wastewater treatment technique based on an aqueous micellar solution has recently received a lot of interest. The aqueous micellar solution approach is a surfactant-based separation technique [18]. Surfactants are nontoxic, nonflammable, and nonvolatile, and they are needed in lower quantities for the aqueous micellar solution process than organic solvents [19]. Surfactants are also amphiphilic compounds that have favorable interfacial characteristics and are frequently used in a variety of industrial separation processes. Nonionic surfactants, in general, do not ionize in an aqueous solution and, at a specific temperature, stimulate the separation of two immiscible aqueous phases [20]. The coacervate phase, which is a surfactant-rich phase, and the diluted phase, which has a reduced surfactant content, are two immiscible aqueous phases, respectively [21]. Figure 1 shows a schematic illustration of CPE.

Beyond the cloud point, many researchers have studied the phase separation of nonionic surfactants. They claimed that micelle attraction, micelle growth, and dehydration of the nonionic surfactant's outer layer's micelles might all contribute to phase separation [22]. The dye is soluble in the micelle's outer layer and core because of the dyes' polarity. The increase in micelle aggregation causes the nonpolar molecules to become solubilized in the micelle core. Due to the dehydration of the polyoxyethylene chains in the mantle, polar molecules are solubilized [22, 23].

The experimental design is typically widely used to optimize a variety of processes, some of which are listed below. (a) Semmoud and Ma [24] carried out factorial design research to improve the Red Bemacid dye concentration during the CPE process by employing ionic liquids. (b) Uranium extraction using Triton X-100 and D2EHPA (2-(2-ethylhexyl)phosphoric acid [25]. (c) A CPE approach with surfactants to effectively eliminate the dye Direct Blue 71 (DB71) from an effluent [26]. (d) Improving the cobalt aluminate synthesis [27]. (e) Predicting the surface stress values of all fluids with a power-law tendency [28].

The process of cloud point extraction (CPE) is often influenced by surfactant concentration and temperature. Therefore, it is important to assess how temperature and surfactant concentration affect the elimination of RB 5. As they enable the consistent optimization of several variables, multivariate approaches have generally been chosen to optimize process parameters like temperature and surfactant concentration [28, 29]. The CPE procedure was previously optimized by altering one parameter while maintaining the values of the other parameters. As a result, the previous optimization method eventually demanded more time and effort and required increased chemical usage to evaluate each parameter. Response surface methodology (RSM) is frequently used to optimize the process variables that directly impact the desired outcome in order to solve this issue. The link between process characteristics and responses is demonstrated by RSM [30, 31]. The RSM method produces findings much more quickly and cheaply than other methods. Additionally, a small number of trials based on factorial designs are used to examine a number of process parameters using RSM. Compared to analytical investigations, RSM has the benefit of being less expensive and time-consuming [32].

To the best of our knowledge, the TX-114-based CPE procedure for RB-5 was limited, and there is no literature on the optimization process parameters used for RB-5. So, in this investigation, the nonionic surfactant TX-114 was used in the cloud point extraction (CPE) method to extract the RB-5 dye. As a result, evaluating the effects of surfactant concentration and temperature on RB-5 removal, optimizing surfactant concentration and temperature for the extraction of the RB-5 dye from an aqueous solution by using RSM, and estimating the phase volume, RB-5 concentration in the dilute phase, and the rich phase after separation, as well as extraction efficiency, are issues that are frequently discussed.

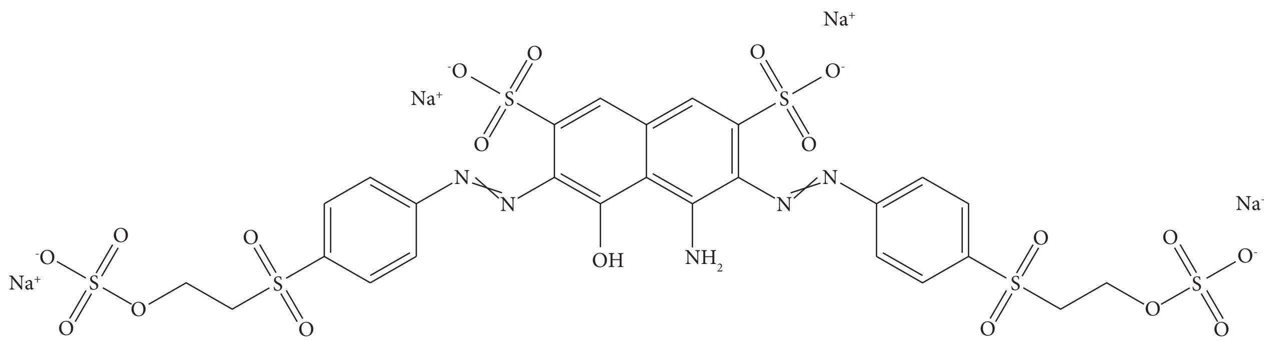

Figure 2: Molecular structure of TX-114.

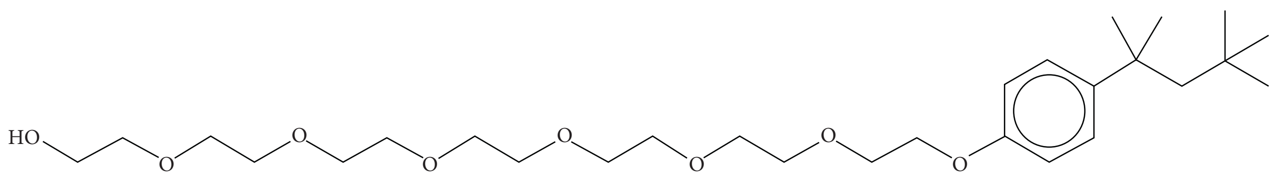

Figure 3: Cloud point of TX-114 with various concentration of RB-5 dye.

2. Materials and Methods

2.1. Materials. Reactive Black-5 (RB-5) dye (molecular formula, $Na_4O_{19}S_6C_{26}H_{21}N_5$) was obtained from Sigma-Aldrich, India. Triton X-114 (t-Octylphenoxy polyoxyethylene ether) was procured from Sigma-Aldrich, India. Chemical structures of RB-5 dye and Triton X-114 are depicted in Figures 2 and 3, respectively. All reagents were used without any further purification.

2.2. Cloud Point Extraction of RB-5 Dye. In textile effluent, color concentrations typically range between 10 and 25 mg·L^{-1}. As a result, different concentrations of Triton X-114 (0.01 M to 0.1 M) and dye (25 ppm, 50 ppm, and 75 ppm) were used to prepare aqueous micellar solutions for this study. Aqueous micellar solutions were kept in a thermostatic bath for 30 minutes as prepared (40, 50, and 60°C, respectively) depending on the cloud point temperature (CPT). (Model: High Precision Thermostatic Water Bath (with Stirrer), The Precision Scientific Co., Chennai, India) [32]. The volumes of the surfactant-rich phase and the diluted phase were recorded after the creation of the heterogeneous clear phases. Then, using a UV-visible spectrophotometer, the concentrations of RB-5 in diluted phases were calculated (Shimadzu, UV-2600).

2.3. Experimental Design. Three levels of factorial design were used: low, medium, and high. The graphs, analysis of variance, and effects computation were all performed using the DESIGN EXPERT 7.0 software program (StateEase, Minneapolis, USA). Various levels of experimental design are depicted in Table 1.

Temperature (X3), dye concentration (X2), and surfactant concentration (X1) were used as parameters, both at the three levels. The mean value served as the experimental response, and the trials were carried out in triplicate. A total of 15 trials were carried out, including one repetition at the central point and 14 connected to the experimental design matrix. Table 2 shows the design matrix and the experimental findings.

Table 1: Various levels of experimental design.

	Symbol	Level		
		−1	0	1
Surfactant concentration (*M*)	X_1	0.01	0.05	0.1
Dye concentration (ppm)	X_2	25	50	75
Operating temperature (°C)	X_3	40	50	60

Temperature and surfactant concentrations were chosen so that they were above the surfactant's turbidity curve, which is shown in Figure 4. Visual observation was used to estimate the cloud point. It was noted that the RB-5 dye plot displayed lower cloud point values. This is caused by how organic molecules interact with the polar head group of surfactants [33].

2.4. Cloud Point Extraction. Experiments with the CPE were carried out, as mentioned in section 2.2. Table 2 lists the experimental data, including the percentage of dye extracted (E), the phase volume ratio (R_v), the concentration of the dye RB-5 in the diluted phase following separation ($X_{s,d}$), and the RB-5 concentration in the surfactant-rich phase following separation ($X_{s,r}$).

2.5. Regression Analysis. A mathematical model was generated using regression analysis. The quadratic polynomial equations that demonstrate the relationship between each response and important variables and iterations are the

Table 2: Experimental results for optimization of RB-5 dye (25 ppm, 50 ppm, and 75 ppm) with TX-114 at various operating temperatures (40°C, 50°C, and 60°C).

				Experimental results				Calculated results			
Test	X_1	X_2	X_3	E (%)	R_v	$X_{s,d}$ (ppm)	$X_{s,r}$ (ppm)	E (%)	R_v	$X_{s,d}$ (ppm)	$X_{s,r}$ (ppm)
1	−1	1	−1	23.923	2.881	0.031	0.455	23.120	2.674	0.042	0.388
2	−1	1	1	34.577	3.734	0.238	0.796	34.910	3.664	0.065	0.739
3	−1	−1	−1	36.389	3.734	0.263	0.897	35.369	4.166	0.301	0.918
4	−1	0	0	36.441	4.384	0.359	0.911	39.632	4.105	0.453	0.967
5	−1	−1	1	63.657	6.383	0.454	0.987	61.955	6.221	0.511	0.949
6	0	0	−1	64.131	12.108	0.480	1.012	64.003	12.253	0.536	1.185
7	0	1	0	67.404	13.636	0.681	1.219	64.568	13.854	0.668	1.208
8	1	1	−1	67.782	15.741	0.795	1.297	69.776	15.745	0.862	1.344
9	0	0	0	72.755	17.924	0.886	1.603	73.144	17.636	0.809	1.621
10	1	1	1	73.381	19.048	0.897	1.819	74.692	18.614	0.879	1.832
11	1	−1	−1	78.961	18.765	1.208	2.020	78.919	19.237	1.142	1.964
12	0	0	1	80.792	24.378	1.222	2.141	79.754	24.061	1.433	2.047
13	0	−1	0	80.992	25.945	1.589	2.528	82.662	27.324	1.533	2.317
14	1	0	0	85.655	30.548	2.453	2.542	81.298	30.023	2.406	2.608
15	1	−1	1	97.536	36.986	2.853	2.864	98.631	36.597	2.832	2.941

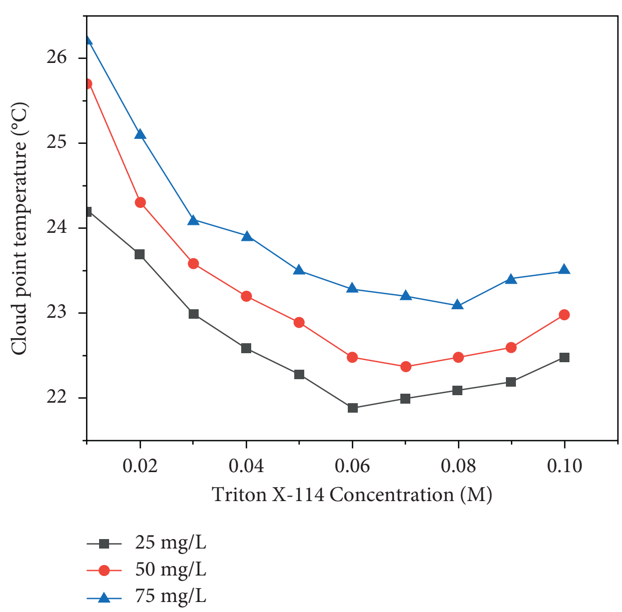

Figure 4: (a) Response surface for dye extraction in (%). (b) Effects of variables on dye extraction in the Pareto chart. (c) Coherence between predicted and observed values of % of extraction.

result of the mathematical model [32]. The models below were derived from experiments.

3. Results and Discussion

3.1. Properties of Dilute Phase and Coacervate Phase. In the supplemental information, the characteristics of the coacervate phase and the dilute phase were covered. The parameters of the diluted phase were determined to be similar to those of water, as given in the additional material in STable 1. The surfactant micelle in the coacervate phase solubilizes the dye that is present in the solution. As a result, the predominant component of the diluted phase is water, and only a very small amount of dye and surfactant are present.

3.2. Statistical Assessment

3.2.1. Analysis of Variance Test. Analysis of variance (ANOVA) was used to determine the validity of the dye extraction model, and the results are shown in Table 3. The correlation measure was also used to calculate the dye extraction model's coefficient of determination (R^2). As can be seen in Table 3, the model demonstrated statistically significant regression with a 95% confidence level ($F_{\text{calculated}}$ greater than F_{tabled}) and an R^2 of 0.9922, revealing that the model represented 99.22% of the variation in the experimental data. It's noteworthy to note that the model's F-value was 140.72, indicating that it was significant and predictive and that there was only a 0.01% possibility that noise was to blame for such a high "model F value."

As demonstrated in Figure 5(a), the temperature had no impact on the dye removal, but the concentration of surfactant had a satisfactory impact. Additionally, Figure 5(a) shows that the interaction between the surfactant and the dye mostly accounted for the fact that the concentration of the surfactant had a stronger impact on the dye extraction efficiency than the temperature. The hydrolytic breakdown of the RB-5 dye is influenced by the ethylene oxide (EO) chains of the surfactant, which form intramolecular or intermolecular hydrogen bonds with dye molecules [34]. Furthermore, the surfactant concentration was higher when the coacervate phase formed, which tends to attach the dye to it regardless of temperature.

The Pareto chart illustrates how the process parameters affected the dye extraction process as presented in Figure 5(b). The surfactant concentration alone had a substantial impact on the model within the 95% confidence interval. This property applies to both the linear and quadratic components. The agreement between the value calculated by the model and the experimental value is shown in Figure 5(c).

Since it directly affects extraction efficiency, surfactant concentration is a crucial factor in CPE [35, 36]. The extraction is only partially effective when the concentration is low, but raising the concentration could affect the outcome of the analysis [37].

Table 3: Validity of dye extraction by ANOVA.

Source	Sum of squares	DF	Mean squares	F_{cal} Value	p value Prob> F	Remark
Reactive Black-5 (E)—$R^2 = 0.9922$						
Regression	6786.40	9	754.04	140.72	< 0.0001	Significant model
Residuals	53.58	10	5.36			
Lack of fit	53.58	5	10.72			
Pure error	0.000	5	0.000			
Total	6839.98	19				
Phase volume ratio (R_v)—$R^2 = 0.9979$						
Regression	1558.72	6	259.79	1014.07	< 0.0001	Significant model
Residuals	3.33	13	0.26			
Lack of fit	3.33	8	0.42			
Pure error	0.0000003	5	0.00000006			
Total	1562.05	19				
RB-5 Concentration in dilute phase ($X_{s,d}$)—$R^2 = 0.9880$						
Regression	9.35	9	1.04	91.85	<0.0001	Significant model
Residuals	0.11	10	0.011			
Lack of fit	0.11	5	0.023			
Pure error	0.000	5	0.000			
Total	9.47	19				
RB-5 Concentration in surfactant rich phase ($X_{s,r}$)—$R^2 = 0.9880$						
Regression	7.87	9	0.87	77.33	< 0.0001	Significant model
Residuals	0.11	10	0.011			
Lack of fit	0.11	5	0.023			
Pure error	0.000	5	0.000			
Total	7.99	19				

Percentage of dye extracted (E) (%):

$$\%E = 73.14 + 20.83X_1 - 9.05X_2 + 7.88X_3 + 0.78X_1X_2 - 1.72X_1X_3 - 3.70X_2X_3 - 12.68X_1^2 + 0.47X_2^2 - 1.27X_3^2. \quad (1)$$

3.2.2. Phase Volume Ratio (R_v). Table 3 indicates the analysis of variance (ANOVA) computations to demonstrate the relevance of the suggested model. 0.9979 was the calculated coefficient of determination. With the appropriate degrees of freedom, the value of the $F_{\text{calculated}}$ test was compared to that of the F_{tabled} test for the F distribution at a 95% confidence level. The proposed model is statistically significant and represents the responses as a function of the examined variables, according to the model F-value of 1014.07. The volume percentage of the coacervate phase increases with an increase in surfactant concentration, according to the response surface depicted in Figure 6(a) [38].

Because the surfactant is less hydrophilic at higher temperatures and creates even more concentrated coacervate in the surfactant, the volume fraction decreases in the temperature scenario. The variables' effects on the coacervate phase volume fraction are depicted in Figure 6(b). The coacervate phase volume fraction is significantly influenced by temperature and surfactant content. Silva et al. [33] showed a similar result for the CPE method's removal of phenol.

It is clear from the concentration of the surfactant that a rise in surfactant concentration will result in a rise in the volume fraction of the coacervate phase. The observations of Ji et al. [35] about similar outcomes during the extraction of phenolic acid from dandelion were also made. Additionally, when the concentration of surfactant rises, more micelles are produced for the CPE process, improving phase separation [39]. Temperature, on the other hand, has a negative impact, suggesting that an increase in this variable would cause a decline in reaction, or a decrease in the volume fraction of the coacervate phase.

Phase volume ratio:

$$Rv = 15.74 + 11.58X_1 + 1.89X_2 - 3.49X_3 + 1.11X_1X_2 - 2.49X_1X_3 - 0.28X_2X_3. \quad (2)$$

3.2.3. Dye Concentration in the Dilute Phase after Separation ($X_{s,d}$). With an R^2 of 0.9880 in Table 3, the suggested model for dye concentration in the diluted phase following separation demonstrated significant regression at a 95% confidence level. The model is suggested to be significant and predictive by the Model F-value of 91.85. A "Model F-value" this large could only happen in 0.01% of cases due to noise, proving the significance and predictability of the suggested model. Figure 7(a) displays the response surface graph made by the suggested model for dye concentration in the separated diluted phase ($X_{s,d}$). This is connected to the extraction efficiency, where the extraction will be lower with less surfactant supplied to the system [35]. The temperature will therefore have no impact on the amount of residual dye present in the aqueous phase following separation because it has no effect on dye extraction. The surfactant, which also serves as an extracting agent in this process, creates the coacervate phase with a substantially equal amount of surfactant once the cloud

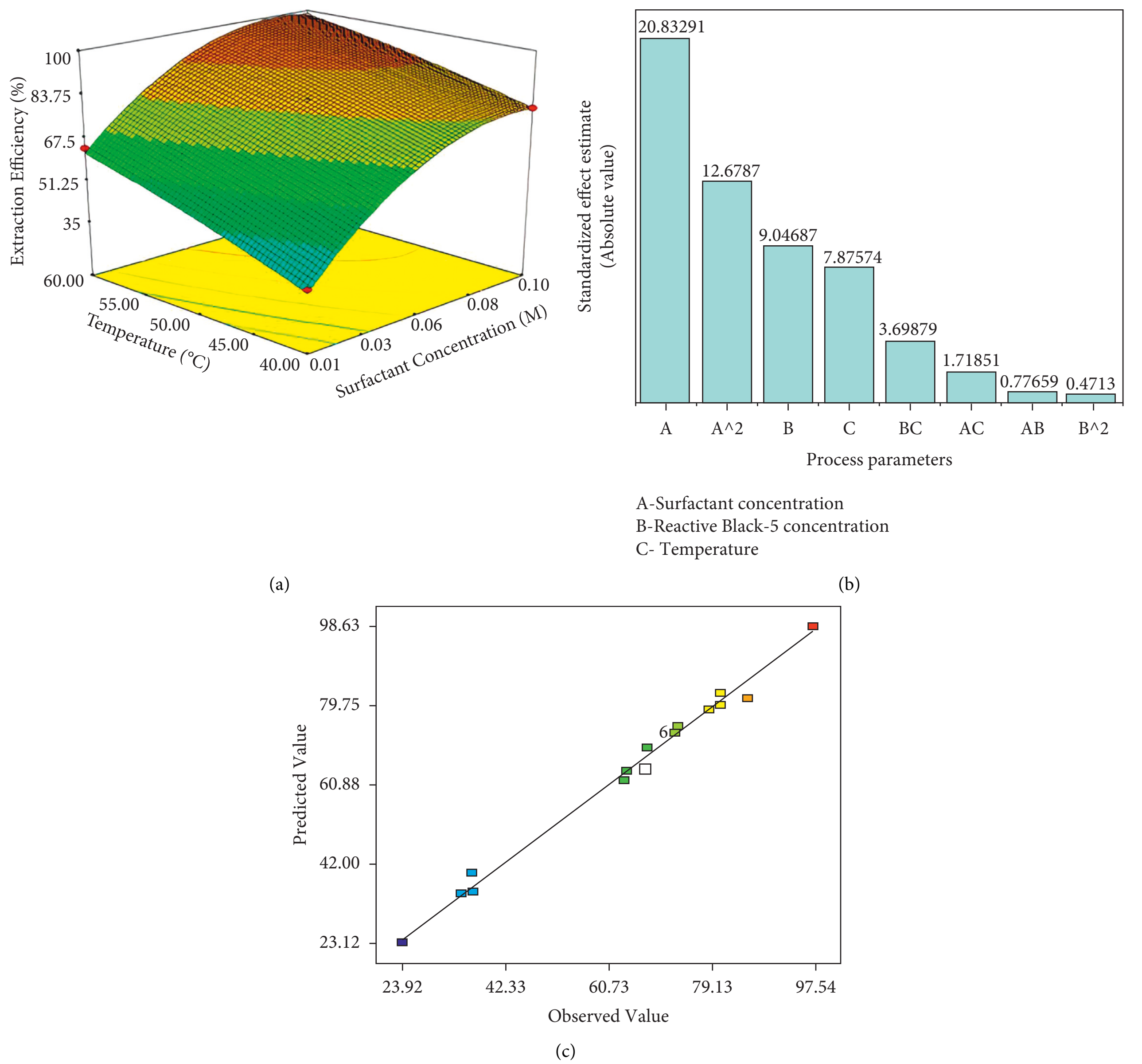

Figure 5: (a) Response surface for the phase volume ratio. (b) Effect of variables on the coacervate phase volume fraction. (c) Relationship between predicted and observed values of the phase volume ratio.

point (turbidity) is reached. This phase is in charge of removing dye from the aqueous phase. Surfactant concentration (linear component) is the significant variable within the 95% confidence interval, as shown by the Pareto chart in Figure 7(b) [33]. On either the linear or the quadratic component, the sole effect of temperature was less significant. The correlation between the experimental data and the values determined by the model is depicted in Figure 7(c).

Dye concentration in the dilute phase after separation ($X_{s,d}$):

$$X_{s,d} = 0.67 - 0.54X1 + 0.68X_2 - 0.17X_3 - 0.28X_1X_2 + 0.023X_1X_3 - 0.019X_2X_3 + 0.32X_1^2 + 0.081X_2^2 + 0.039X_3^2. \quad (3)$$

3.2.4. Dye Concentration in the Surfactant-Rich Phase after Separation ($X_{s,r}$). After phase separation, the residual dye concentration in the surfactant-rich phase is a crucial factor in determining the feasibility of the operation. Even though the extraction efficiency is high, the procedure is no longer practical due to the rising dye concentration since the loss of surfactant in the treated effluent leads to cost escalation and effluent contamination. The analysis of variance (ANOVA) was used to determine the model's applicability in predicting residual dye concentration, and the results are shown in Table 4 with an R^2 value of 0.9858. With the appropriate degrees of freedom, the value of the $F_{\text{calculated}}$ test was compared to that of the F_{tabled} test for the F distribution at a 95% confidence level. The model is suggested to be significant and predictive by the model F-value of 77.33. A "Model *F*-value" this large might happen owing to noise only 0.01%

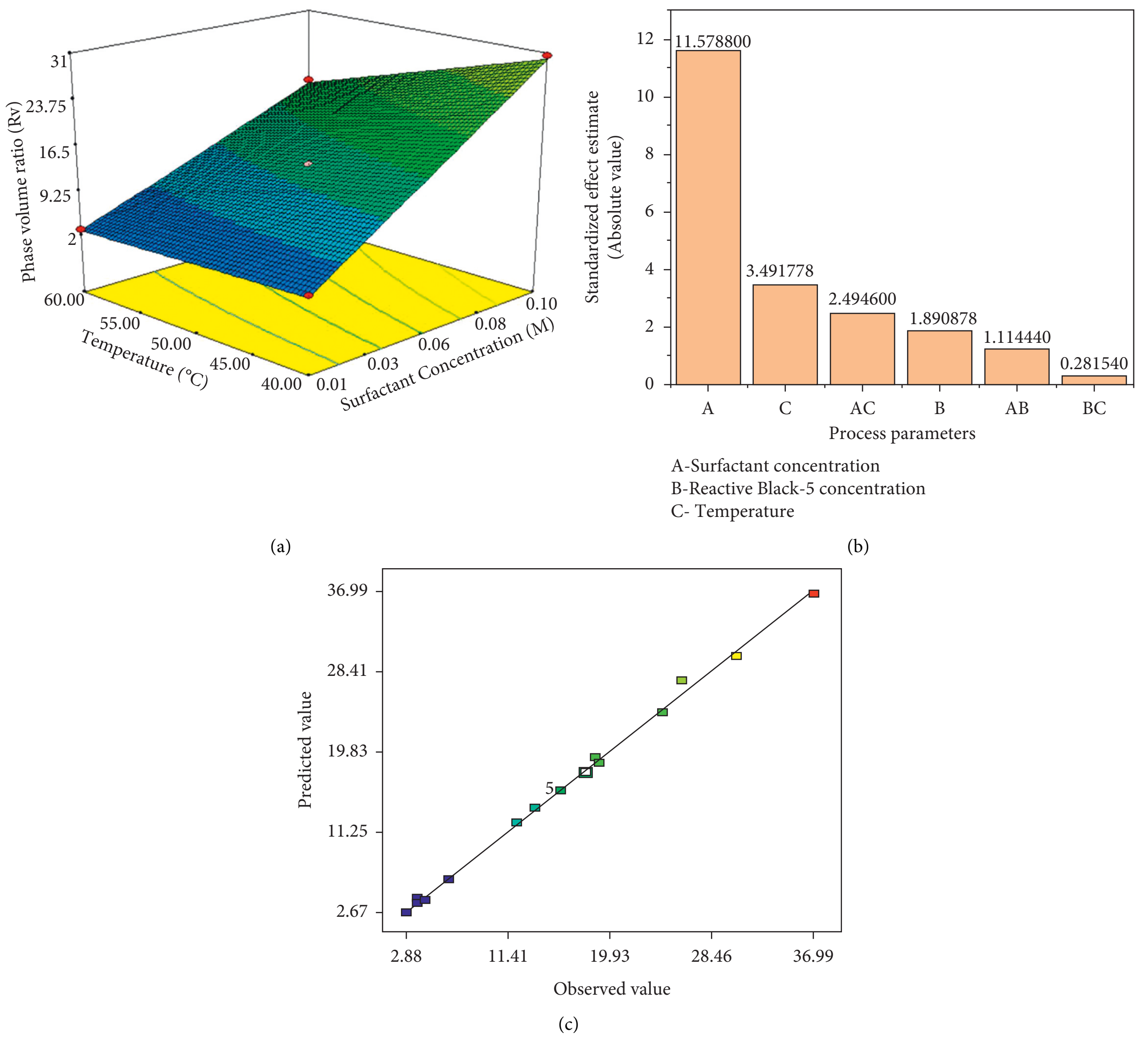

FIGURE 6: (a) Response surface for dye concentration in the dilute phase after separation. (b) Pareto chart for dye concentration in the dilute phase after separation. (c) Comparison between predicted and observed values of dye concentration in the dilute phase after separation.

of the time. Response surface plots are depicted in Figure 8(a), showing the impacts of temperature and dye concentration. Within the examined range, as temperature rises, there is a propensity to obtain progressively lower dye concentrations in the surfactant-rich phase. The concentration of the surfactant-rich phase rises as the dye concentration does as well. The hydrophilicity of the surfactant decreases with temperature, which decreases its concentration in the aqueous phase. The initial dye concentration and temperature were shown to have significant impacts at a 95% confidence interval, according to the Pareto chart shown in Figure 8(b), which was produced by statistically analyzing experimental data. As a result, after separation, larger dye concentrations result from an increase in concentration in the surfactant-rich phase. After separation, the surfactant-rich phase has lower dye concentration values due to the rise in temperature. It is mostly caused by a rise in temperature because it intensifies micellar interactions [38, 40], and [41]. The consistency of the findings is demonstrated in Figure 8(c) by the correlation between experimental data and model predictions.

The response surface approach and experimental design were crucial for optimizing and examining the impact of temperature and surfactant concentration on RB-5 dye extraction. The outcome of the current investigation demonstrated that the efficiency of the process is influenced by both the temperature and concentration of the surfactant.

Dye concentration in the surfactant-rich phase after separation ($X_{s,r}$):

$$X_{s,r} = 1.83 + 0.54X_1 + 0.57X_2 + 0.17X_3 + 0.28X_1X_2 - 0.023X_1X_3 + 0.019X_2X_3 - 0.32X_1^2 + 0.081X_2^2 - 0.039X_3^2. \quad (4)$$

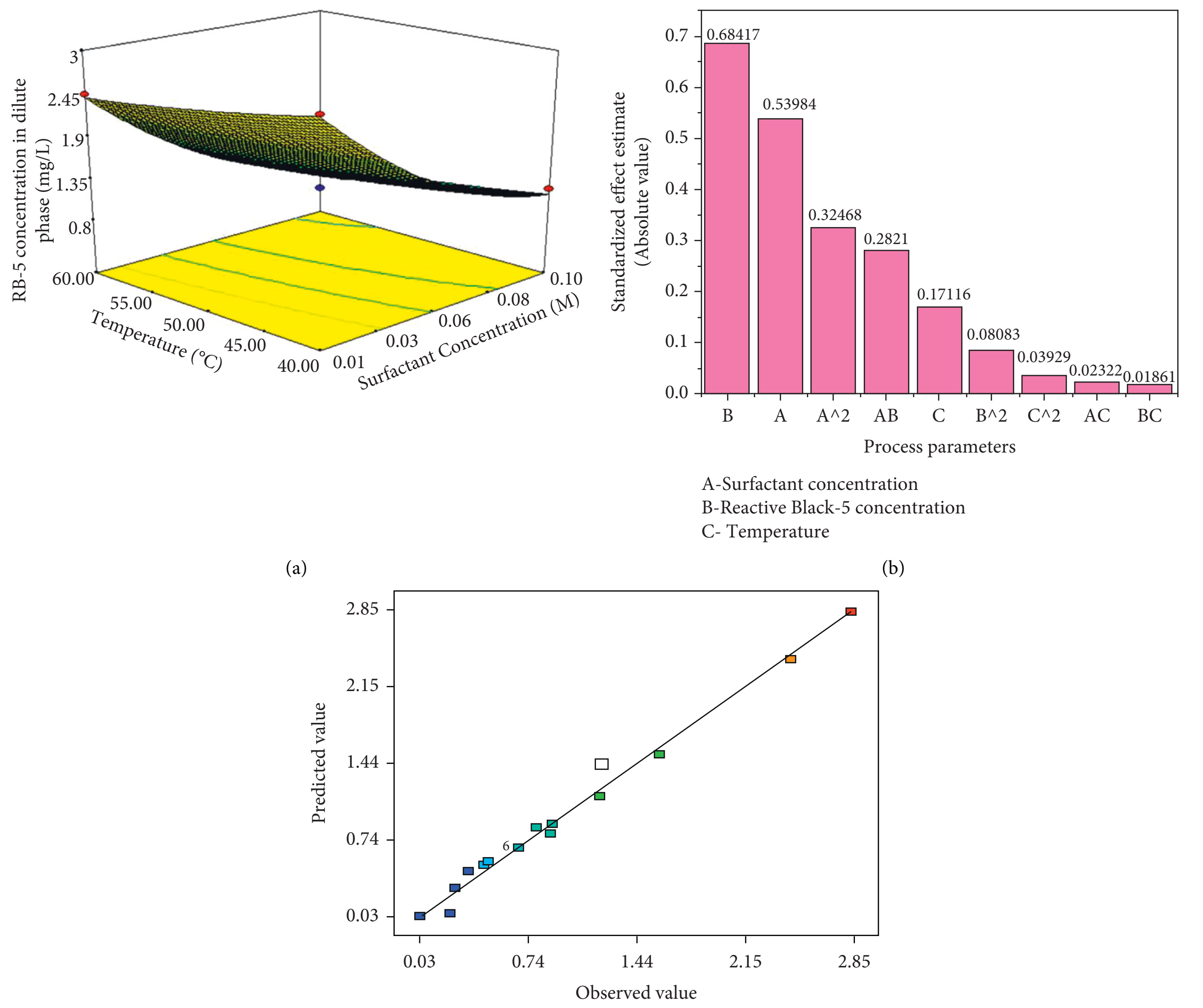

Figure 7: (a) Response surfaces for dye concentration in the surfactant-rich phase. (b) Pareto chart for dye concentration in the surfactant-rich phase. (c) Relationship between predicted values of dye concentration in the surfactant-rich phase and the observed value.

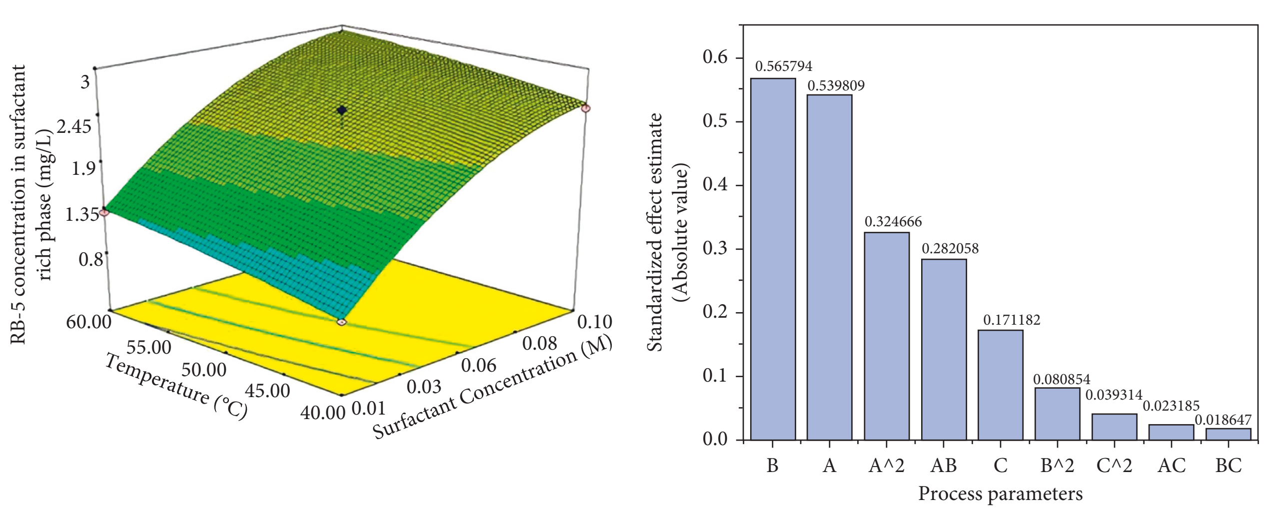

Figure 8: Continued.

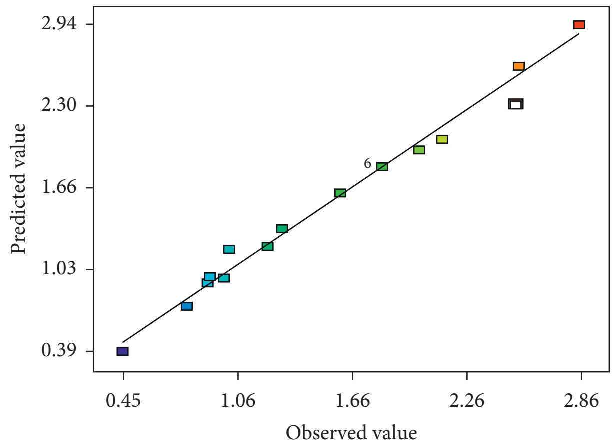

(c)

Figure 8: (a) Response surfaces for dye concentration in the surfactant-rich phase. (b) Pareto chart for dye concentration in the surfactant-rich phase. (c) Relationship between predicted values of dye concentration in the surfactant-rich phase and the observed value.

Table 4: Regression statistics.

Phase volume ratio	
R^2	0.9979
Adjusted R^2	0.9969
Predicted R^2	0.9905
Standard deviation	0.5061
Mean	15.74
RB5 concentration in dilute phase	
R^2	0.9880
Adjusted R^2	0.9773
Predicted R^2	0.9083
Standard deviation	0.1064
Mean	0.8907
RB5 concentration in rich phase	
R^2	0.9858
Adjusted R^2	0.9731
Predicted R^2	0.8913
Standard deviation	0.1064
Mean	1.61

4. Conclusion

In this study, the experimental design and RSM were used to assess the impact of surfactant concentration and temperature on the dye extraction parameters. The obtained results showed that the process efficiency is highly influenced by both parameters, such as temperature and surfactant concentration. In this instance, surfactant concentration increases the efficiency of the extraction process, the phase volume ratio, and the dye concentration of the surfactant-rich phase while decreasing the dye concentration in the diluted phase. Temperature, however, has no impact on the effectiveness of the extraction process or the dye concentration in the diluted phase following separation. Only the volume ratio of the coacervate phase is affected by temperature, and as the temperature rises, the volume ratio of the coacervate phase decreases. Overall, the findings of the present investigation showed that 0.1 M surfactant at 60°C produces successful dye extraction with 98% removal (see Table 4).

Data Availability

The excel data will be available on request from the corresponding author. The excel data will be available on request from the corresponding author.

Conflicts of Interest

The authors declare that there are no conflicts of interest.

Acknowledgments

Dr. Sathish Kumar Ramachandran and Dr. Duraimurugan alias Saravanan Dhanabalan thank the Department of Chemical Engineering, National Institute of Technology, Tiruchirappalli 620015, Tamil Nadu, India, for laboratory support in conducting this study.

Supplementary Materials

S1. Physical properties of surfactant dilute phase and surfactant-rich phase. *Table S1*. Physical properties for 75 ppm (RB-5- TX-114) of surfactant dilute phase and surfactant-rich phase at 313.15 K, 323.15 K, and 333.15 K. *Table S2*. Physical properties for 50 ppm of surfactant dilute phase and surfactant-rich phase at 313.15 K, 323.15 K, and 333.15 K. *Table S3*. Physical properties for 25 ppm of surfactant dilute phase and surfactant-rich phase at 313.15 K, 323.15 K, and 333.15 K. *S1.1*. Variation of refractive index with TX-114 concentration. *S1.2*. Variation of density with TX-114 concentration. *S1.3*. Variation of viscosity with TX-114 concentration. (*Supplementary Materials*)

References

[1] D. A. Yaseen and M. Scholz, "Textile dye wastewater characteristics and constituents of synthetic effluents: a critical review," *International journal of Environmental Science and Technology*, vol. 16, no. 2, pp. 1193–1226, 2019.

[2] N. Daneshvar, A. Oladegaragoze, and N. Djafarzadeh, "Decolorization of basic dye solutions by electrocoagulation: an investigation of the effect of operational parameters," *Journal of Hazardous Materials*, vol. 129, no. 1–3, pp. 116–122, 2006.

[3] T. Adane, A. T. Adugna, and E. Alemayehu, "Textile industry effluent treatment techniques," *Journal of Chemistry*, vol. 2021, Article ID 5314404, 14 pages, 2021.

[4] S. J. Kulkarni, "Environment friendly synthesis of colour, pigment and dyes: a review," *International Journal of Research and Review*, vol. 4, no. 4, pp. 19–23, 2017.

[5] E. Narbona, J. C. del Valle, M. Arista, M. L. Buide, and P. L. Ortiz, "Major flower pigments originate different colour signals to pollinators," *Frontiers in Ecology and Evolution*, vol. 9, pp. 1–14, 2021.

[6] B. Lellis, C. Z. Fávaro-Polonio, J. A. Pamphile, and J. C. Polonio, "Effects of textile dyes on health and the environment and bioremediation potential of living organisms," *Biotechnology Research and Innovation*, vol. 3, no. 2, pp. 275–290, 2019.

[7] S. S. Affat, "Classifications, advantages, disadvantages, toxicity effects of natural and synthetic dyes: a review clinical chemistry view project journal of global pharma Technology view project," *University of Thi-Qar Journal of Science*, vol. 8, no. 1, pp. 130–135, 2021.

[8] M. El Bouraie and W. S. El Din, "Biodegradation of Reactive Black 5 by Aeromonas hydrophila strain isolated from dye-contaminated textile wastewater," *Sustainable Environment Research*, vol. 26, no. 5, pp. 209–216, 2016.

[9] J. Marszałek and R. Żyłła, "Recovery of water from textile dyeing using membrane filtration processes," *Processes*, vol. 9, no. 10, p. 1833, 2021.

[10] H. Singh, G. Chauhan, A. K. Jain, and S. K. Sharma, "Adsorptive potential of agricultural wastes for removal of dyes from aqueous solutions," *Journal of Environmental Chemical Engineering*, vol. 5, no. 1, pp. 122–135, 2017.

[11] E. Oyarce, K. Roa, A. Boulett et al., "Removal of dyes by polymer-enhanced ultrafiltration: an overview," *Polymers*, vol. 13, pp. 3450–19, 2021.

[12] M. S. Momina, M. Shahadat, and S. Isamil, "Regeneration performance of clay-based adsorbents for the removal of industrial dyes: a review," *RSC Advances*, vol. 8, no. 43, pp. 24571–24587, 2018.

[13] M. F. Sevimli and C. Kinaci, "Decolorization of textile wastewater by ozonation and Fenton's process," *Water Science and Technology*, vol. 45, no. 12, pp. 279–286, 2002.

[14] S. P. Azerrad and E. Kurzbaum, "Chemical decolorization of textile wastewater via advanced oxidation processes: case study of key parameters with acid blue 25," *Water, Air, and Soil Pollution*, vol. 232, no. 2, p. 40, 2021.

[15] G. Sandeepgovardhan, A. Divyakala, D. Bhargav, V. R. Praveen, and G. Ramohan, "Decolorization of dye waste water by activated carbon," *Global Journal of Research and Review*, vol. 7, no. 2, pp. 59–65, 2020.

[16] H. Biglari, S. RodrigueziCouto, Y. O. Khaniabadi et al., "Cationic surfactant-modified clay as an adsorbent for the removal of synthetic dyes from aqueous solutions," *International Journal of Chemical Reactor Engineering*, vol. 16, no. 5, pp. 1–14, 2018.

[17] R. Al-Tohamy, S. S. Ali, F. Li et al., "A critical review on the treatment of dye-containing wastewater: ecotoxicological and health concerns of textile dyes and possible remediation approaches for environmental safety," *Ecotoxicology and Environmental Safety*, vol. 231, Article ID 113160, 2022.

[18] M. Topf, T. Ingram, T. Mehling, T. Brinkmann, and I. Smirnova, "Product recovery in surfactant-based separation processes: pervaporation of toluene from concentrated surfactant solutions," *Journal of Membrane Science*, vol. 444, pp. 32–40, 2013.

[19] A. C. Leite, A. M. Ferreira, E. S. Morais, I. Khan, M. G. Freire, and J. A. P. Coutinho, "Cloud point extraction of chlorophylls from spinach leaves using aqueous solutions of nonionic surfactants," *ACS Sustainable Chemistry & Engineering*, vol. 6, no. 1, pp. 590–599, 2018.

[20] L. Zhao, X. Zhang, and Z. Wang, "Extraction of anionic dyes with ionic liquid–nonionic surfactant aqueous two-phase system," *Separation Science and Technology*, vol. 52, no. 5, pp. 804–811, 2017.

[21] F. K. G. Santos, E. L. B. Neto, M. C. P. A. Moura, T. N. C. Dantas, and A. A. D. Neto, "Molecular behavior of ionic and nonionic surfactants in saline medium," *Colloids and Surfaces A: Physicochemical and Engineering Aspects*, vol. 333, no. 1–3, pp. 156–162, 2009.

[22] J. A. Molina-Bolívar, J. Aguiar, and C. C. Ruiz, "Growth and hydration of triton X-100 micelles in monovalent alkali salts: a light scattering study," *Journal of Physical Chemistry B*, vol. 106, no. 4, pp. 870–877, 2002.

[23] K. Pytlakowska, V. Kozik, and M. Dabioch, "Complex-forming organic ligands in cloud-point extraction of metal ions: a review," *Talanta*, vol. 110, pp. 202–228, 2013.

[24] R. Semmoud and D. Ma, "Cloud point extraction of toxic red Bemacid dye by ionic liquids and nonionic surfactant system and factorial design," *Academic Journal of Engineering Studies*, vol. 1, no. 4, pp. 1–8, 2020.

[25] N. T. Sanaa, M. A. Didi, and D. Villemin, "Uranium micelle-mediated extraction in acetate medium: factorial design optimization," *Journal of Radioanalytical and Nuclear Chemistry*, vol. 293, no. 3, pp. 789–795, 2012.

[26] M. Alibrahim, "Cloud point extraction of direct blue 71 dye using triton X-100 as nonionic surfactant," *Tenside Surfactants Detergents*, vol. 58, no. 1, pp. 27–32, 2021.

[27] Y. F. Gomes, P. Medeiros, M. Bomio et al., "Optimizing the synthesis of cobalt aluminate pigment using fractional factorial design," *Ceramics International*, vol. 41, no. 1, pp. 699–706, 2015.

[28] K. Muthamizhi, P. Kalaichelvi, S. T. Powar, and R. Jaishree, "Investigation and modelling of surface tension of power-law fluids," *RSC Advances*, vol. 4, no. 19, pp. 9771–9776, 2014.

[29] S. L. C. Ferreira, M. A. Bezerra, W. N. L. Dos Santos, and B. B. Neto, "Application of Doehlert designs for optimisation of an on-line preconcentration system for copper determination by flame atomic absorption spectrometry," *Talanta*, vol. 61, no. 3, pp. 295–303, 2003.

[30] T. Mutuk and B. Mesci, "Analysis of mechanical properties of cement containing boron waste and rice husk ash using full factorial design," *Journal of Cleaner Production*, vol. 69, pp. 128–132, 2014.

[31] D. B. Muñiz-Márquez, J. E. Wong-Paz, J. C. Contreras-Esquivel, R. Rodriguez-Herrera, and C. N. Aguilar, "Extraction of phenolic compounds from coriandrum sativum L. And *Amaranthus hybridus* L. By microwave Technology," in *Polyphenols in Plants*, pp. 185–190, Elsevier, Amsterdam, Netherlands, 2019.

[32] D. F. Melvin Jose, R. Edwin Raj, B. Durga Prasad, Z. Robert Kennedy, and A. Mohammed Ibrahim, “A multi-variant approach to optimize process parameters for biodiesel extraction from rubber seed oil,” *Applied Energy*, vol. 88, no. 6, pp. 2056–2063, 2011.

[33] W. P. N. Silva, A. E. G. d. Nascimento, M. C. P. D. A. Moura, H. N. M. d. Oliveira, and E. L. d. Barros Neto, “Study of phenol removal by cloud point extraction: a process optimization using experimental design,” *Separation and Purification Technology*, vol. 152, pp. 133–139, 2015.

[34] J. Wang, Y. Zhang, H. Dou, and L. Pei, “Influence of ethylene oxide content in nonionic surfactant to the hydrolysis of reactive dye in silicone non-aqueous dyeing system,” *Polymers*, vol. 10, no. 10, p. 1158, 2018.

[35] Y. Ji, L. Wu, R. Lv, H. Wang, S. Song, and M. Cao, “Facile cloud point extraction for the separation and determination of phenolic acids from dandelion,” *ACS Omega*, vol. 6, no. 20, pp. 13508–13515, May 2021.

[36] F. Rasoolzadeh, P. Hashemi, and F. Nazari Serenjeh, “Ionic liquid-based cloud-point extraction of quercetin for its sensitive HPLC–UV determination in juice samples,” *Acta Chromatographica*, vol. 29, no. 4, pp. 493–496, 2017.

[37] N. I. Mohd, M. Raoov, S. Mohamad, and N. N. M. Zain, “Performance evaluation of non-ionic silicone surfactants OFX 0309 and DC 193C as a new approach in cloud point extraction—spectrophotometry for determination of atrazine in water samples,” *RSC Advances*, vol. 8, no. 24, pp. 13556–13566, 2018.

[38] A. Appusamy, P. Purushothaman, K. Ponnusamy, and A. Ramalingam, “Separation of methylene blue dye from aqueous solution using triton X-114 surfactant,” *Journal of Thermodynamics*, vol. 2014, Article ID 670186, 16 pages, 2014.

[39] Y. Zhong, H. Wang, and K. Diao, “Densities and excess volumes of binary mixtures of the ionic liquid 1-butyl-3-methylimidazolium hexafluorophosphate with aromatic compound at T=(298.15 to 313.15)K,” *The Journal of Chemical Thermodynamics*, vol. 39, no. 2, pp. 291–296, Feb. 2007.

[40] A. Appusamy, I. John, K. Ponnusamy, and A. Ramalingam, “Removal of crystal violet dye from aqueous solution using triton X-114 surfactant via cloud point extraction,” *Engineering Science and Technology, an International Journal*, vol. 17, no. 3, pp. 137–144, 2014.

[41] Y. Lin, X. He, G. Han, Q. Tian, and W. Hu, “Removal of Crystal Violet from aqueous solution using powdered mycelial biomass of Ceriporia lacerata P2,” *Journal of Environmental Sciences*, vol. 23, no. 12, pp. 2055–2062, 2011.